M. A. BIOT *Shell Development Company, Houston, Texas*

Theory of Folding of Stratified Viscoelastic Media and Its Implications in Tectonics and Orogenesis

M. A. BIOT
H. ODÉ
W. L. ROEVER
Shell Development Company, Houston, Texas

Experimental Verification of the Theory of Folding of Stratified Viscoelastic Media

Geological Society of America Bulletin, v. 72, p. 1595–1632, 13 figs., November 1961

M. A. BIOT
H. ODÉ
W. L. ROEVER
Shell Development Company, Houston, Texas

Experimental Verification of the Theory of Folding of Stratified Viscoelastic Media

Abstract: An experimental check has been obtained for the stability theory of stratified viscoelastic media in compression. Model tests have been conducted for both an elastic layer and a viscous layer embedded in a viscous medium and subject to a compression parallel with the layer. The appearance of the folds and the measured wavelengths are in good agreement with the theoretical predictions. For a better interpretation of the tests, the writers present a theoretical evaluation of the time history of deformation for a layer whose folding develops from a given initial departure from perfect flatness. The calculated folding of the layer at various intervals is plotted for different values of the significant parameter.

CONTENTS

1. INTRODUCTION AND ACKNOWLEDGMENTS

Biot (1957; 1959a; 1959b) has described theoretical analyses of the folding of a viscoelastic layer under compression in a viscoelastic medium. The particular cases of a viscous or elastic layer in a viscous medium have been rederived and discussed by elementary methods in a companion paper (Biot, 1961). The writers here establish an experimental verification of these results by model tests in the laboratory. The tests covered the cases of both the elastic layer and the viscous layer embedded in a viscous medium. It may be assumed that such simplified models embody the significant aspects of the physics and furnish a crucial check of the theory.

To prepare adequately the qualitative, as well as the quantitative, interpretation of the tests, the writers evaluate the time history of the folding from the theory. Since folding cannot occur in a geometrically perfect plane layer, the writers have introduced an initial disturbance in the form of a kink and have calculated the subsequent deformation and development of folds that appear as a result of compression in the layer. This is accomplished in sections 2 and 3. Only the case of a viscous layer was evaluated. The theory indicates that similar results will be obtained for an elastic layer. The appearance of the dominant wave-

Geological Society of America Bulletin, v. 72, p. 1621–1632, 7 figs., 2 pls., November 1961

length and the qualitative aspect of the folds predicted by the theory are well verified by the tests. The experiments are described in Section 4, their results discussed in Section 5. Results for the elastic layer show good agreement with the theoretical prediction regarding the dependence of the dominant wavelength on the compression load and its independence of the viscosity of the medium. Satisfactory agreement is also obtained for the case of a viscous layer, in which the dominant wavelengths are close to the calculated values and are independent of the compression loads, as predicted.

The authors wish to acknowledge the valuable assistance of Mr. T. J. Shankland in the experimental phase of this work.

2. ANALYTICAL EVALUATION OF THE TIME HISTORY OF FOLDING

Consider the case of a viscous layer of thickness h embedded in an infinite viscous medium (Fig. 1). The layer is under an initial compression P per unit area. In the companion paper, Biot (1961) derived an equation for the lateral deflection, w, of the layer[1] and investigated the stability of the layer. He restricted the analysis to an infinite wave of constant wavelength. He found that an initial sinusoidal deflection, w, of the layer, represented by

$$w = W_0 \cos lx \,, \tag{2.1}$$

increases exponentially with time. After a time t, the deflection (2.1) becomes[2]

$$w = W_0 e^{pt} \cos lx \,, \tag{2.2}$$

where

$$p = \frac{P}{\dfrac{4\eta_1}{hl} + \dfrac{1}{3}\eta h^2 l^2} \tag{2.3}$$

(h = thickness of the layer, η_1 = viscosity coefficient of the medium, η = viscosity coefficient of the layer).

The wavelength L is related to l by

$$L = \frac{2\pi}{l} \,. \tag{2.4}$$

In the present analysis, this result will be used to solve a more complex problem. Instead of starting with an initial deflection (2.1) that is perfectly sinusoidal, the writers will consider the case in which the initial deflection, $w_0(x)$, is localized. The problem will then be to evaluate the time history of the folding under the compression P. This can be done by using the principle of superposition. The initial deflection can be represented as a superposition of cosine functions by a Fourier integral. Consider an initial deflection represented by the expression

$$w_0(x) = \frac{b}{1 + \left(\dfrac{x}{a}\right)^2} \,. \tag{2.5}$$

This is a bell-shaped curve, as Figure 2 shows. Expression (2.5) can be written as a Fourier integral by the well-known identity

$$\frac{b}{1 + \left(\dfrac{x}{a}\right)^2} = ba \int_0^\infty e^{-la} \cos lx \, dl \,. \tag{2.6}$$

For any given wavelength, any sinusoidal component under the integral sign will be multiplied by the factor e^{pt}, as expressed by equation (2.2). The deflection $w(x,t)$ after a time t is thus obtained by multiplying each component under the integral sign in equation (2.6) by this factor, *i.e.*,

$$w(x,t) = ba \int_0^\infty e^{pt-la} \cos lx \, dl \,. \tag{2.7}$$

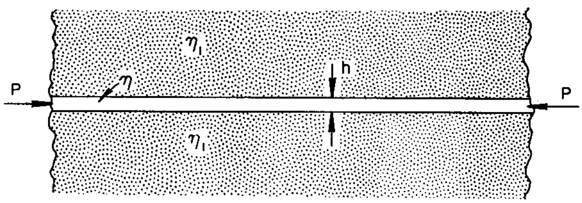

Figure 1. Layer of thickness h and viscosity η under compressive stress P in a medium of viscosity η_1

[1] The equation was also derived as a particular case of a more elaborate theory (Biot, 1957).

[2] *See* equation (4.11) of the companion paper (Biot, 1961).

The quantity p is a function of l, given by equation (2.3).

The computation of this integral was done numerically. It is convenient to make use of the time t_1 already introduced in earlier work (Biot, 1959a; 1959b; 1961):

$$t_1 = \frac{\eta}{P}. \tag{2.8}$$

As pointed out, t_1 is the time required for the layer to shorten by 25 per cent if it remained straight while under the constant pressure P. In this case, L_d is independent of the load. For viscosity ratios $\eta/\eta_1 = 1000$ and 144, $L_d = 34.57\ h$ and $18.12\ h$, respectively. On the other hand, the average wave number of the initial perturbation can be defined as

$$l_{\text{av.}} = \frac{\int_0^\infty l e^{-la}\, dl}{\int_0^\infty e^{-la}\, dl} = \frac{1}{a}, \tag{3.2}$$

so that the average wavelength, $L_{av.}$, of the initial perturbation is, by equations (2.4) and (3.2),

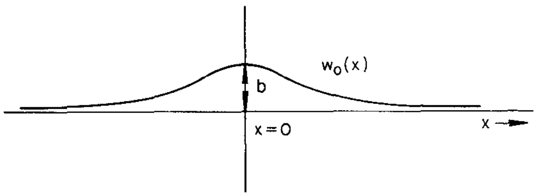

Figure 2. Shape of assumed initial disturbance of the layer

It is convenient to use t_1 as a reference time. In the calculations and in plotting the results, the writers will represent the time by means of the dimensionless ratio t/t_1. The method used for the numerical evaluation of the integral (2.7) is explained in the Appendix.

3. NUMERICAL EVALUATION OF THE TIME HISTORY OF FOLDING

Let us consider the parameters and variables of the problem. As shown by equation (A.2) in the Appendix, the deflection w is a function of a/h, t/t_1, and the viscosity ratio η/η_1. It is also proportional to the maximum initial deflection, b. Computations were carried out for three values of the viscosity ratio, but results are presented in detail only for the two values $\eta/\eta_1 = 1000$ and 144, since these adequately point out the significant features. For each ratio, three different values of the parameter a/h were so chosen that the average wavelength content of the initial perturbation is related in a definite way to the physically dominant wavelength of the system. The latter is the wavelength of fastest rate of growth under a given load P. It tends to obliterate all others. As shown earlier (Biot, 1957; 1959a; 1961), the dominant wavelength for the present case is given by

$$L_d = 2\pi h \sqrt[3]{\frac{\eta}{6\eta_1}}. \tag{3.1}$$

$$L_{\text{av.}} = 2\pi a\,. \tag{3.3}$$

For the computation, a was so chosen that, approximately,

$$L_d = \frac{1}{2} L_{\text{av.}}, L_{\text{av.}}, 2L_{\text{av.}}\,. \tag{3.4}$$

From equations (3.1), (3.3), and (3.4), the values of a/h corresponding to equation (3.4) can be computed. They are, approximately,

$$a/h = 11, 5.50, 2.75 \tag{3.5}$$

for the ratio $\eta/\eta_1 = 1000$, and

$$a/h = 5.60, 2.80, 1.50 \tag{3.6}$$

for $\eta/\eta_1 = 144$.

The three cases (3.5) for the viscosity ratio $\eta/\eta_1 = 1000$ are plotted in Figure 3. The shape of the deformed layer is plotted at various instants. The abscissa represents the ratio x/h of the distance x along the layer to the thickness h. The deformation is symmetric with respect to the origin because the initial perturbation is symmetric about this point. Hence, only the deformation on one side of the axis of symmetry is shown ($x > 0$). The ordinates are proportional to the deflections of the layer but do not represent the actual magnitude. The point of maximum deflection is on the axis of symmetry ($x = 0$), and all deflections at that point are reduced to the same value, taken as unity. The graphs therefore show the gradual development of the folds of a half-portion of the layer. The shape of the layer is shown at four instants—at $t = 0$, where the shape is the initial disturbance in the ratio 1:4. This introduces very little difference in the time history of the folding. A definite wavelength is measurable that is very close to the dominant wavelength, $L_d = 34.57\ h$.

A similar plot is shown in Figure 4 for the

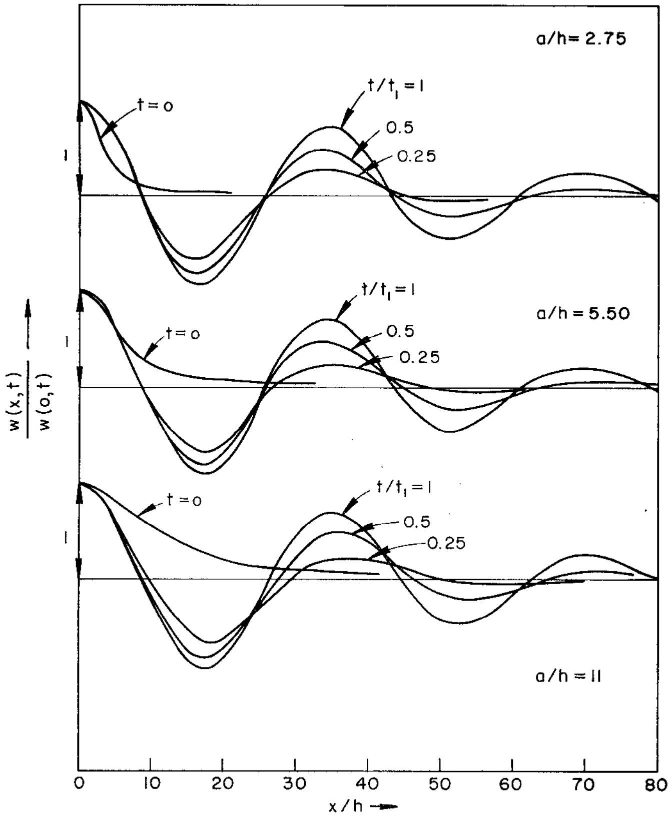

Figure 3. Time history of folding for a viscosity ratio $\eta/\eta_1 = 1000$. Three types of initial disturbances (at $t = 0$) are considered. All amplitudes are reduced to unity at the center ($x = 0$). Only the right half of the symmetric figure is shown.

assumed initial disturbance itself as represented by equation (2.5), and subsequently at

$$t = 0.25t_1,\ 0.50t_1, \text{ and } t_1\,. \tag{3.7}$$

The magnitude of the deflection at any point is known, once it has been calculated at $x = 0$. This is discussed hereafter.

Figure 3 also indicates that after sufficient time a very definite wavelength appears that is quite sharp. The three values of a/h for which the deflections have been evaluated correspond to a variation of the width of the three cases in which the viscosity ratio $\eta/\eta_1 = 144$ (3.6); here also, the curves have been plotted for the instants (3.7).

Again, the result is fairly insensitive to the width of the initial disturbance. Although the definition in this case is less sharp, a characteristic wavelength appears that is close to the dominant wavelength, $L_d = 18.12\ h$, at least in the later phase of the folding. The observed wavelength in this case tends to shift slightly toward longer waves when the width of the initial perturbation increases.

We shall now consider the amplitude of the folding. We must evaluate the amplitude on the axis of symmetry of the initial disturbance, *i.e.*, at $x = 0$. The initial deflection at that point is equal to b. At time t, it is found by putting $x = 0$ in equation (2.7); *i.e.*,

$$w(0,t) = ba \int_0^\infty e^{pt-la}\, dl\,. \tag{3.8}$$

In Figure 5, we have plotted the ratio $w(0,t)/b$, for a purely sinusoidal deformation of dominant wavelength. The amplification factor A_d is given by equation (5.15) of Biot (1961):

$$\log A_d = \frac{t}{t_1}\left(\frac{\eta}{6\eta_1}\right)^{2/3}, \tag{3.9}$$

where log is the natural logarithm.

Figures 3 and 4 confirm the conclusions of Biot's analysis (1961) regarding band width

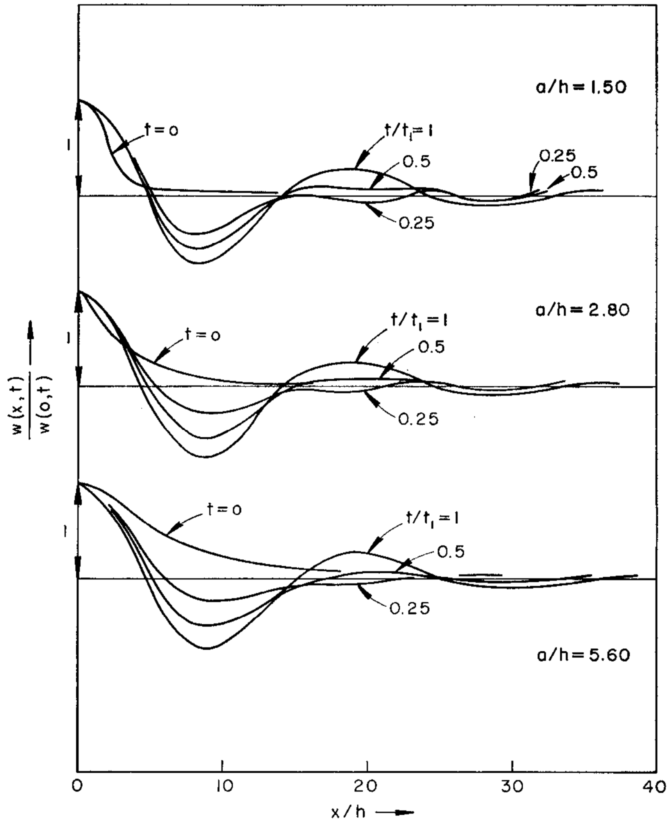

Figure 4. Time history of folding for a viscosity ratio $\eta/\eta_1 = 144$. Three types of initial disturbances (at $t = 0$) are considered. All amplitudes are reduced to unity at the center ($x = 0$). Only the right half of the symmetric figure is shown.

i.e., the amplification factor at $x = 0$ as a function of t/t_1, for the values of the viscosity ratio η/η_1 and a/h given heretofore.

It can be verified that the amplification given by equation (3.8) is not very sensitive to the width of the initial perturbation and that it is closely approximated by the amplification factor A_d, which Biot (1961) derived and selectivity of the folding. Biot found that regular waves can be expected to appear over a distance

$$D = \frac{L_d}{\Delta l/l_d}$$

when $\Delta l/l_d$ is the band width as given by Table 2 of the Biot (1961) paper. For an

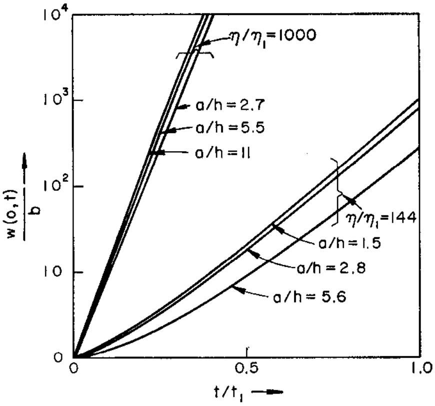

Figure 5. Amplitude $w(0, t)$ at the center ($x = 0$) for the time histories shown in Figures 3 and 4 (b = amplitude at the center of the initial disturbance)

amplification factor $A_d = 1000$, this yields the value$\Delta l/l_d = 0.632$, indicating that $D = 1.58$ L_d. As shown by Figure 5 for the case in which $\eta/\eta_1 = 1000$, the amplification $A_d = 1000$ corresponds to $t/t_1 \cong 0.3$. Figure 3 shows that folding at this instant is regular over a distance of about 1.5 L_d, as calculated. We must, of course, consider the fact that the figure shows only half of the complete picture.

The significance of these results can be illustrated by a specific example. Consider a layer of thickness $h = 2$ feet and viscosity $\eta = 10^{21}$ cgs. This layer is subject to a compression $P = 1450$ psi and is embedded in a medium of viscosity $\eta_1 = 10^{18}$ cgs. The initial deflection is assumed to correspond to $a/h = 5.50$ (hence, $a = 11$ feet), and its maximum value at the center is shown as $b = 0.24$ inch. The time t_1 is

$$t_1 = \frac{\eta}{P} = 319{,}000 \text{ years}.$$

The folding deformation of this layer at the time

$$t = 0.3t_1 = 95{,}700 \text{ years}$$

can be derived from Figures 3 and 5. Figure 6 shows the shape and amplitude. The maximum amplitude at the center is

$$w(0, t) \cong 1000b = 20 \text{ feet}.$$

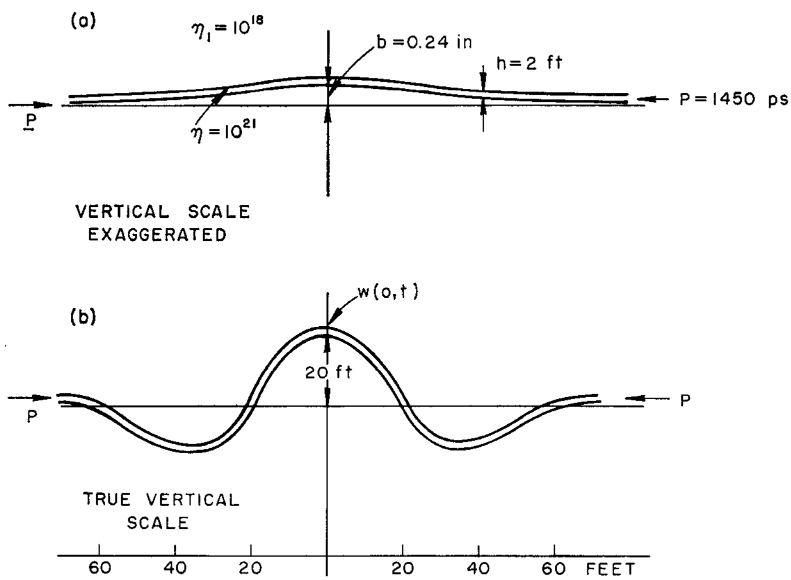

Figure 6. Example of folding of a viscous layer in a viscous medium. (a) layer of thickness $n = 2$ feet with initial disturbance of maximum amplitude $b = 0.24$ inch under horizontal compression $P = 1450$ psi. (b) deformation and folding of the layer after 95,700 years. At that time, the amplitude of folding is 20 feet at the center. (The figure does not take into account the shortening between crests due to the geometry of folding at finite amplitude. *See* Section 6 of Biot's (1961) companion paper.)

The analysis presented is based on the assumption of an initial bell-shaped disturbance, represented by equation (2.5). A much more complicated type of initial irregularity can be represented by a superposition of bell-shaped curves of various widths and locations. The resulting deformation of the layer is then obtained by superposition of the folding due to each initial bell-shaped component. Time histories with such composite initial disturbances were evaluated. The results do not differ significantly from those given heretofore, except for the very special case in which the spacing of the disturbances is such that the folds tend to cancel each other by being exactly out of phase.

At the larger amplitudes of folding, the rate of folding becomes much slower than predicted by the present linear theory. This is due to a nonlinear effect of geometric origin. Therefore, the folding amplitudes will tend to equalize and exhibit more regular behavior at large strain, as already pointed out by Biot (1961).

Time histories for the case of an elastic layer or for problems with more complex viscoelastic properties can be computed by the same method. As shown by the previous analysis of band width, the folding for the elastic layer can be expected to show more regularity of the waves. This conclusion is borne out by the model tests discussed in the following section.

4. DESCRIPTION OF EXPERIMENTS

Laboratory tests of the buckling theory have been conducted for two cases—an elastic layer in a viscous medium, and a viscous layer in a viscous medium. As derived previously (Biot, 1957), the dominant wavelength for an elastic layer in a viscous medium is

$$L_d = \pi h \sqrt{\frac{E}{(1 - \nu^2)P}}, \tag{4.1}$$

where E and ν are Young's modulus and Poisson's ratio of the layer, respectively; the dominant wavelength for the viscous layer is given by equation (3.1).

The tests were designed to verify these formulas and to show that the type of deformation observed conforms with the predictions of the previous sections.

The experiments were performed in a tank 1 m high, 1 m wide, and 20 cm front to back. A narrow plate-glass window was provided in the center of the front and back for observation and photography. The tank was filled with the viscous medium, and the layers were lowered into it in a vertical position and were compressed vertically by weights (Pl. 1). Weights were placed on a platform that moved vertically on guide rails above the tank. Application of the load to the layer tripped a microswitch, which started the clock used to read loading time to fractions of a second. Another clock, used to read to the nearest second, was started manually.

Results were observed photographically by a 35-mm Robot camera with spring-loaded rapid film advance. With this device, up to five pictures per second could be taken. An attempt was made to record still faster deformations with a 16-mm movie camera. At these higher deformation rates, the inertial forces become important in the experiment, and the theory is no longer applicable.

Corn syrup was chosen as the viscous medium because it has relatively high viscosity at room temperature and is transparent, water soluble, nontoxic, and inexpensive. Two grades of syrup manufactured by the Corn Products Company were used—their most viscous grade, No. 1152, and a less viscous grade, No. 1132.

A locally obtained grade of roofing tar was selected for the viscous layers because it could be readily cast into shape and yet was sufficiently viscous so that the layers could be handled into and out of the tank. The mold was lined with thin sheets of Teflon, which enabled the cast layers to be removed from the mold without damage. Elastic layers were made of sheet aluminum and of cellulose acetate butyrate, which were chosen primarily on the basis of availability.

The viscosity of the two grades of syrup was determined both by using a Hoeppler viscometer and by timing the rate of fall of ball bearings through the syrup and applying the Stokes law. These measurements were in close agreement and are summarized in Table 1.

The quantity $E/(1 - \nu^2)$ was obtained for the aluminum and cellulose acetate butyrate layers by direct measurement from the bending of small strips, approximately 2 cm by 10 cm, cut from the sheets. Each strip was measured in two ways—as a cantilever beam loaded at the end, and as a beam freely supported on the ends and loaded in the center. The strip was assumed to be sufficiently wide in relation to its thickness (20 to 1 minimum) to bend as a plate into a cylindrical surface. In that case, the effective modulus used in the

TABLE 1. DIMENSIONS AND CONSTANTS USED

Material	Viscosity (poises)	Density
Pitch (25° C)	3.0×10^7	1.253
1132 corn syrup (24.8° C)	7.0×10^2	1.4
1152 corn syrup (24.9° C)	1.35×10^4	1.45

Sheet used	Thickness h (cm)	Width (cm)	$E/(1 - \nu^2)$ (dynes/cm^2)	Viscosity (poises)
Cellulose acetate butyrate	0.102	19.72	1.25×10^{10}	
	0.0787	19.72	1.76×10^{10}	
	0.0510	19.72	2.42×10^{10}	
	0.0254	19.72	2.43×10^{10}	
Aluminum	0.0531	19.70	5.79×10^{11}	
Pitch	0.35	19.70		3.0×10^7
	0.37	19.70		3.0×10^7
	0.87	19.70		3.0×10^7
	1.08	19.70		3.0×10^7

standard beam formulas is $E/(1 - \nu^2)$. Results of these measurements, which agreed within $\pm$ 20 per cent, are averaged together and are summarized in Table 1.

The viscosity of the tar was determined by a standard method, called the rod-viscometer method, which involves the shearing of a 2-cm by 2-cm by 10-cm beam of the material (Saal, 1933).

From measurements with several different loads, the rate of deformation was found to be proportional to the applied load, indicating true Newtonian behavior. In addition, no yield point was apparent, since the material would eventually flow to a plane surface under the influence of gravity.

The measurement subject to the largest error in these experiments is that of the wavelength of the buckling. The method used here was merely to measure the distance from the first

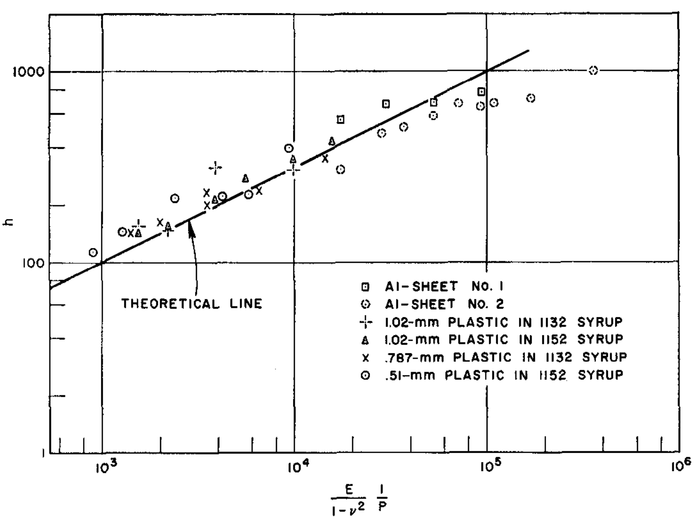

Figure 7. Graph of results of buckling of elastic layers in a viscous medium. L_d = measured wavelength; h = layer thickness; P = compressive load; E = Young's modulus of layer; ν = Poisson's ratio of layer.

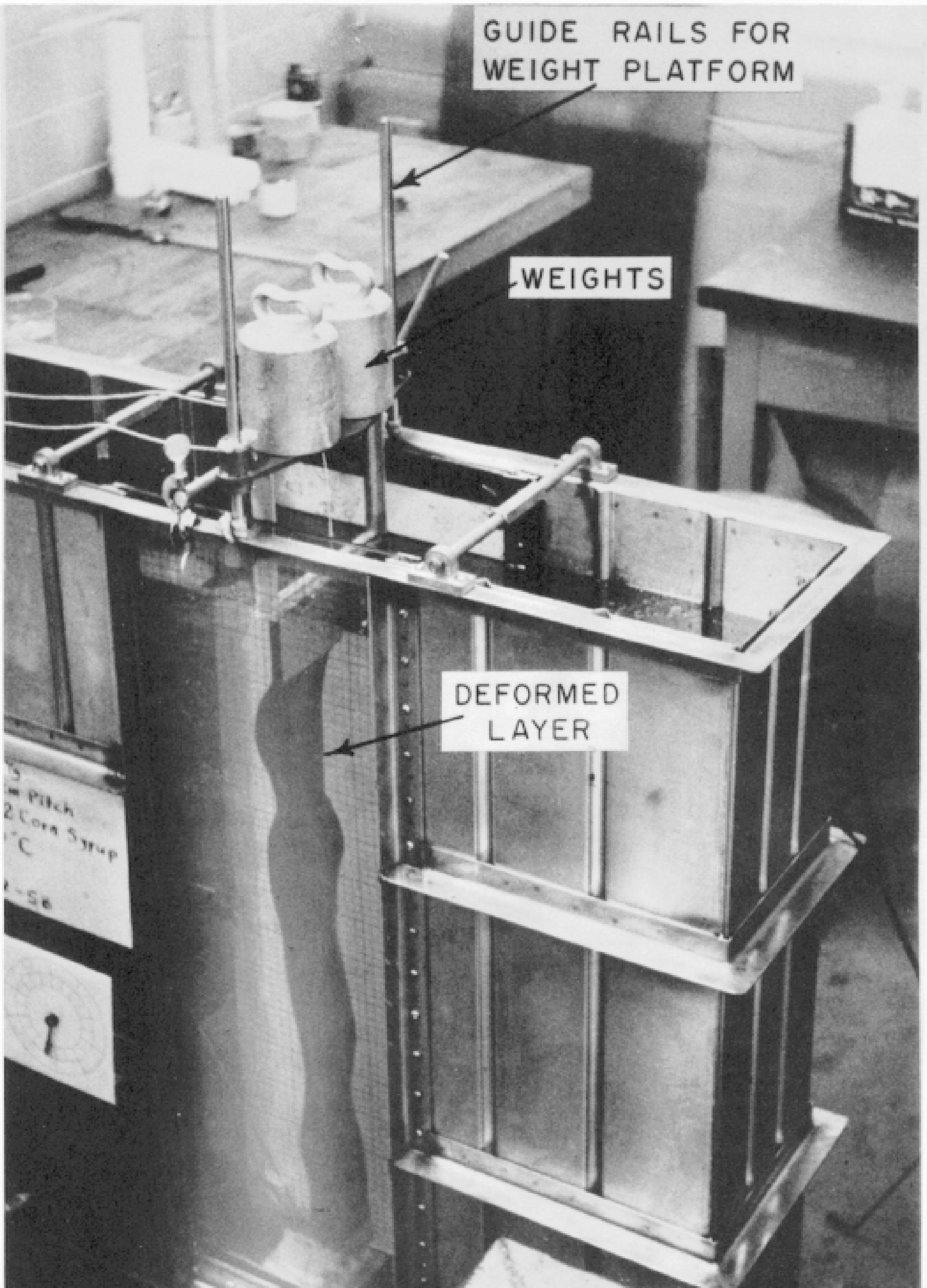

DEFORMATION TANK

BIOT, ODÉ, AND ROEVER, PLATE 1
Geological Society of America Bulletin, volume 72

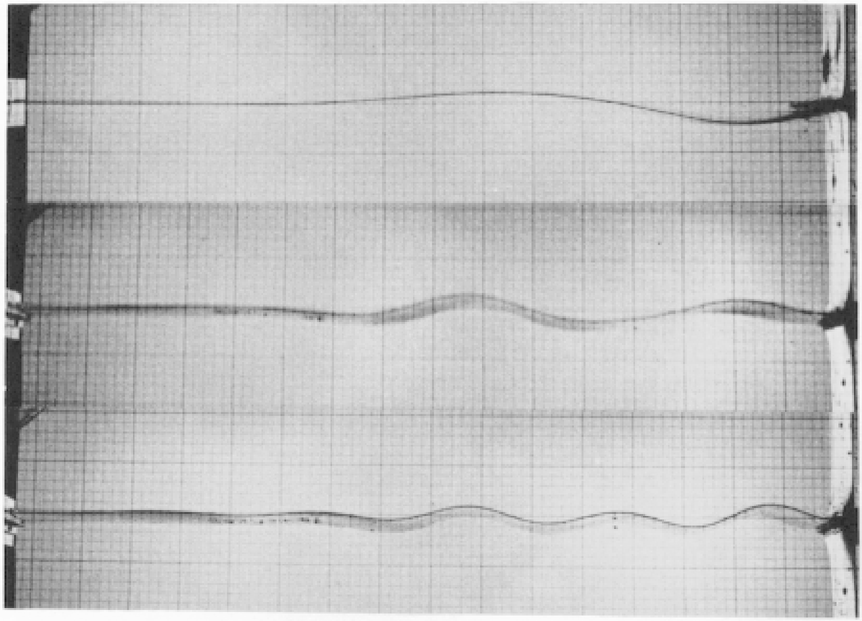

Figure 1

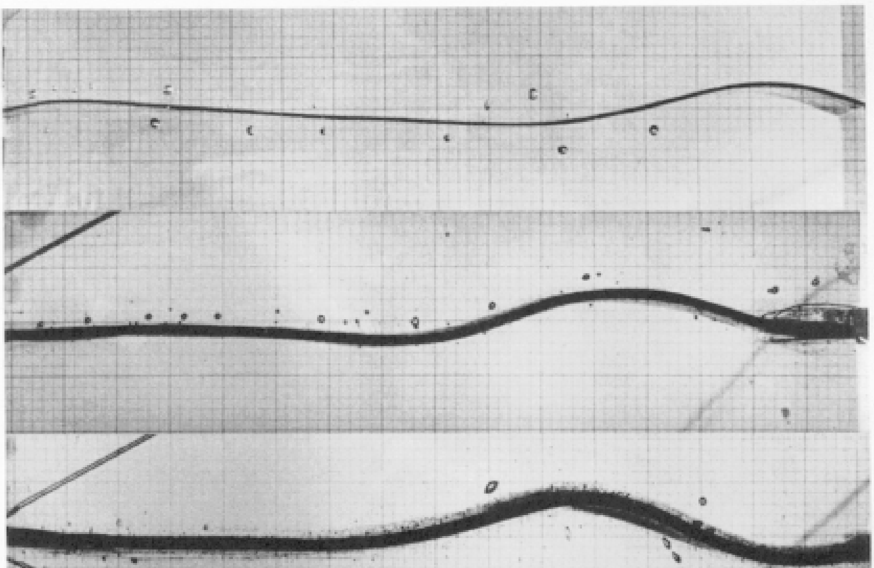

Figure 2

ELASTIC AND VISCOUS LAYERS BUCKLING IN A VISCOUS MEDIUM peak or trough to the last (a centimeter scale is superposed on each photograph) and divide by the number of cycles observed. This was very straightforward in the case of the elastic layers (Pl. 2, fig. 1), in which a number of well-defined peaks and troughs existed, but became somewhat more ambiguous in the case of the viscous layers, in which the buckling damped out rapidly away from the end where the load was applied (Pl. 2, fig. 2). In all cases, however, the writers attempted to measure the distance between the better developed peaks and troughs and to average these measurements to obtain the wavelength used in the results.

TABLE 2. DEPENDENCE OF WAVELENGTH ON VISCOSITY RATIO

η_1 (poises)	η/η_1	h (cm)	L_d/h (calc.)	L_d/h (exp.)
700	4.28×10^4	0.37	121.0	119 – 127
1.35×10^4	2.22×10^3	0.35	45.1	35.3 – 51.4
1.35×10^4	2.22×10^3	0.87	45.1	39.1 – 47.1
1.35×10^4	2.22×10^3	1.08	45.1	35.2 – 48.1

5. DISCUSSION OF EXPERIMENTAL RESULTS

Results for the elastic layer are shown in Figure 7. The ratio of dominant wavelength to layer thickness is plotted against E/P $1 - \nu^2)$, where E is Young's modulus, P is the compressive stress, and ν is Poisson's ratio. The results demonstrate the predicted dependence of wavelength upon load over most of the range but show more deviation at longer wavelengths. This is in the region in which the observed wavelength is influenced by the length of the layer used in the experiments, which will be discussed presently.

Elastic layers were buckled in both of the viscous media (viscosity ratio approximately 20) with no consistent change in observed wavelength, as predicted by the theory.

Experiments with the layers under an initial long bend showed that the observed wavelength was influenced by the preset bend whenever the expected value was within about one to one-half times the preset bend. Shorter wavelengths, however, simply superimposed themselves upon the longer bends with no change in observed wavelength from previous initially undistorted cases.

A much smaller number of experiments were made with viscous layers. One set of four experiments was made to demonstrate the predicted dependence of wavelength on viscosity ratio (Table 2). Another set of experiments was performed in which the load was varied by a factor of 4. This did not change the wavelength, which is in accord with the theory.

To obtain an idea of the magnitude of the amplification involved in these tests, we can compute A_d from equations (2.8) and (3.9). For the folding shown in Figure 2A of Plate 2, $P = 2.153 \times 10^5$ dynes/cm², $t/t_1 = 0.054$, and $\eta/\eta_1 = 4.28 \times 10^4$, so that $A_d = 92$. For the folding shown in Figure 2C of Plate 2, $P = 5.348 \times 10^5$ dynes/cm², $t/t_1 = 0.339$, and $\eta/\eta_1 = 2.22 \times 10^3$, so that $A_d \cong 44$. These

PLATE 2. ELASTIC AND VISCOUS LAYERS BUCKLING IN A VISCOUS MEDIUM

Figure 1. Buckling of elastic layers in a viscous medium under various loads. 1-mm acetate layer in 1132 corn syrup. (A) 1.6-kg load; (B) 6.6-kg load; (C) 11.6 kg- load. All loads applied from right side.

Figure 2. Buckling of viscous layers in a viscous medium

	Load (kg)	Time applied (sec)	Layer thickness (cm)	η/η_1
A	1.6	7.5	0.37	40,000
B	11.6	49	0.87	2,000
C	11.6	19	1.08	2,000

All loads applied from right side

values appear to be reasonable, since they imply an initial waviness of the layer having an amplitude of the order of 1 mm or less.

There are several obvious difficulties in these experiments. In the first place, the boundary condition of an infinite layer and a surrounding medium is far from attained. Friction occurs as the edge of the plate is forced to shear a thin layer of fluid between the sheet and the glass windows. The extent to which this friction affects the results was not evaluated. Other difficulties with boundary conditions occur in cases in which the dominant wavelength is longer than about half the depth of the tank, because the ends of the plate have to be restrained, thereby forcing nodes. For this reason, whenever possible, measurements were made in the range in which the wavelength was less than half the length of the layer. In addition, with very thin plates it was necessary to clamp the upper and lower ends, thus imposing a zero slope at the end nodes.

Secondly, the various layers suffered from defects of one kind or another. The aluminum was slightly prestressed and tended to assume a single wavelength. The plastic sheets, especially the thinnest ones, had an inherent transverse bend, which increased the effective rigidity. To counteract this tendency, the writers clamped the ends.

The tar layers were less dense than the syrup and hence floated unless restrained. Since they would eventually deform and flow from any clamp, a different kind of restraint was necessary. Before the tar was cast, two strings were run down the length of the mold so that they occupied a position as near as possible to the neutral fiber. When the tar layer was in the tank, the strings were tied to a weight at the bottom; after the run, they were used to lift the tar from the tank. Nonetheless, they must have increased the stiffness of the tar and, to some extent, must have altered its experimental behavior.

Thirdly, the insertion of very thin sheets into the syrup invariably distorted the sheets; in the case of the thinnest tar layer in the thickest syrup, the sheets were distorted irreparably.

The results from these rather crude experiments seem to show surprisingly good quantitative agreement with the theory, but a somewhat more elegant experiment might show more dramatic results. Particularly, an experiment that uses as the viscous medium a material of sufficiently high viscosity that it can be handled as a solid with the layer cast inside it might circumvent many of the difficulties encountered in these experiments. However, this method would lose the advantage of repeatability inherent in the present technique, in which the same layer can be deformed several times.

REFERENCES CITED

Biot, M. A., 1957, Folding instability of a layered viscoelastic medium under compression: Royal Soc. London Proc., ser. A, v. 242, p. 444–454

——— 1959a, On the instability and folding deformation of a layered viscoelastic medium in compression: Jour. Applied Mechanics, ser. E, v. 26, p. 393–400

——— 1959b, Folding of a layered viscoelastic medium derived from an exact stability theory of a continuum under initial stress: Applied Mathematics Quart., v. XVII, no. 2, p. 185–204

——— 1961, Theory of folding of stratified viscoelastic media and its implications in tectonics and orogenesis: Geol. Soc. America Bull., v. 72, p. 1595–1620

Filon, N. L., 1928, On a quadrature formula for trigonometric integrals: Royal Soc. Edinburgh Proc., ser. A, v. 49, p. 38–47

Saal, R. N. J., 1933, Determinations regarding the plastic properties of asphaltic bitumen: 1st World Petroleum Cong. (London) Proc., pt. II, p. 515–523

Manuscript Received by the Secretary of the Society, May 9, 1960

APPENDIX: EVALUATION OF THE INTEGRAL (2.7)

By putting

$$s = lh\,, \tag{A.1}$$

we can write the integral (2.7) as

$$\frac{w(x,t)}{b} = \frac{a}{h}\int_0^\infty \exp \left[\frac{-as}{h} + \frac{t}{t_1} f^{-1}(s)\right] \cos\left(\frac{sx}{h}\right) ds\,, \tag{A.2}$$

in which

$$f(s) = \frac{4\eta_1}{s\eta} + \frac{1}{3}s^2\,. \tag{A.3}$$

For a given value of t/t_1, the factor exp $[(-as/h) + (t/t_1) f^{-1}(s)]$, considered as a function of s, is replaced by straight-line intervals.

Equation (A.2) then becomes

$$\frac{w(x,t)}{b} = \frac{a}{h}\sum^{k} \int_{A_k}^{A_{k+1}} (a_k s + b_k) \cos\left(\frac{sx}{h}\right) ds$$

$$= \frac{a}{h}\sum^{k}\left[(a_k s + b_k)\frac{\sin(xs/h)}{x/h}\Bigg|_{A_k}^{A_{k+1}} + \frac{a_k}{(x/h)^2}\cos\frac{xs}{h}\Bigg|_{A_k}^{A_{k+1}}\right],$$

in which a_k and b_k are given for the interval. Because $a_k A_{k+1} + b_k = a_{k+1}A_{k+1} + b_{k+1}$, all but two terms due to the first bracketed term disappear; those also disappear, however, because $\sin(xs/h)/(x/h)$ tends to zero for s vanishing, and $a_k s + b_k$ tends to zero for k tending to infinity. Thus,

$$\frac{w(x,t)}{b} = \frac{a}{h}\sum^{k}\frac{a_k}{(x/h)^2}\cdot\left(\cos A_{k+1}\frac{x}{h} - \cos A_k\frac{x}{h}\right).$$

For small values of x, this expression has to be expanded into powers of x. The method used here for the computation of integrals of the type (A.2) was first proposed by Filon (1928).